

Scientific Computing Exercise Set 3

Michael MacFarlane Glasow (12317217) & Anezka Potesilova (15884392) & Tycho Stam (13303147)

Repository: https://github.com/kingilsildor/CLS-Scientific_Computing-Assignment3

I. INTRODUCTION

DIFFUSION has a wide range of applications. While having previously studied diffusion over time, eigenvalues and eigenmodes of membranes will guide this investigation, in order to study what these values can reveal about the underlying structure of a system. The concept of resonance is of particular interest in structural engineering, where resonances are actively avoided in the design, as oscillations can lead to devastating consequences. Fostering further understanding of how resonance and systems interact is therefore worth investigating.

This investigation will study how membranes resonate under specific conditions. The different parts of the system oscillate together at the same frequency, leading the investigation to the analysis of how the shape of the membranes influences the oscillating frequencies [1]. One application of eigenmodes is analysing different boundary layers in fluid dynamics. In this case, an eigenmode is the natural vibration of a system.

Iterative methods as well as direct methods will be implemented in order to study the phenomena mentioned. Initially, the eigenvalues and eigenmodes of various shapes will be examined using iterative solving methods. Then, the phenomena will be studied with direct solving technique, in order to solve for the concentration. Finally, the leapfrog method will be implemented for simple one-dimensional harmonic oscillators.

The report is structured as follows: In the Theory section, the equations describing our model are introduced as well as the eigenvalue problem and the matrix form. Furthermore, in the Methods section, the discretization and numerical schemes and methods for solving these are given as well as any initial conditions and further considerations. In the Results, we show the results of our simulations using various visualisation methods while specifying how the results were obtained. Lastly, in the Discussion section, we go through the results and comment on them while mentioning any limitations and concluding.

Hereby we derived the following research questions:

- *How does the spectrum of eigenfrequencies depend on the size L ?*

- *How does the eigenmodus evolve over time?*
- *How do Dirichlet boundary conditions impact steady-state diffusion?*
- *How can we increase the convergence without an increase in cost?*
- *How does the behaviour of an oscillator change for different frequencies of the driving force?*

II. THEORY

TO understand how different membranes resonate, the two-dimensional wave equation will be considered:

$$\frac{\partial^2 u}{\partial t^2} = c^2 \nabla^2 u$$

With the solution form:

$$u(x, y, t) = v(x, y, t)T(t) \quad (1)$$

Whereby the equation is split into a spacial and temporal part, as specified by the assignment. When doing this the temporal part can be transformed into an eigenvalue problem:

$$\nabla^2 v(x, y) = Kv(x, y) \quad (2)$$

The solution of which will result in the eigenfrequencies λ by the following equation:

$$\begin{aligned} \lambda^2 &= -K \\ \lambda &= \sqrt{-K} \end{aligned}$$

To find a solution for this, v will be discretized resulting in a set of linear equations in the form of:

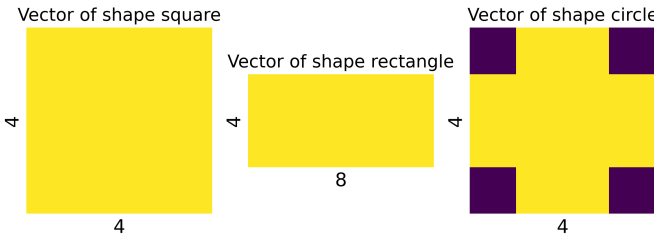
$$\mathbf{M}\mathbf{v} = \mathbf{K}\mathbf{v} \quad (3)$$

Where \mathbf{M} is a matrix and \mathbf{v} is a vector representing the unknowns. Based on the assignment description, the following three membrane shapes will be considered, with $L \in [10, 200]$, The shapes of which can be seen in Figure 1.

- a square with side length L
- a rectangle with sides L and $2L$
- a circle with diameter L

For the temporal component, an oscillating solution will occur when $K < 0$, resulting in:

$$T(t) = A \cos(c\lambda t) + B \sin(c\lambda t) \quad (4)$$

Fig. 1: Different membrane shapes for $L = 4$.

Hereby, A represents the initial position of $T(t)$ at the start, and B the initial velocity. Within this report, the assumption is made that $A = 1$ and $B = 1$, for easier calculations. Following the previously mentioned identity, $\lambda > 0$ can be assumed without loss of generality, as stated by the assignment.

For finding the solution for the steady-state solution, the temporal element is no longer applicable. The solution will be expressed as $Mc = b$. First, a matrix for ∇^2 will be constructed, identically as described above. For this exercise, we will focus on the circular domain of radius 2. The Dirichlet boundary conditions will be implemented in the following manner. We modified the system matrix to disregard all points outside of the domain such that the corresponding rows in the matrix were zeroed out and the diagonal was set to one. This ensures that $c = 0$ is observed on the boundary.

A simple one-dimensional harmonic oscillator can be modelled as an object attached to a spring that is governed by the following equations:

$$\frac{dx}{dt} = v \quad (5)$$

$$\frac{dv}{dt} = \frac{F(x)}{m} = -\frac{kx}{m} \quad (6)$$

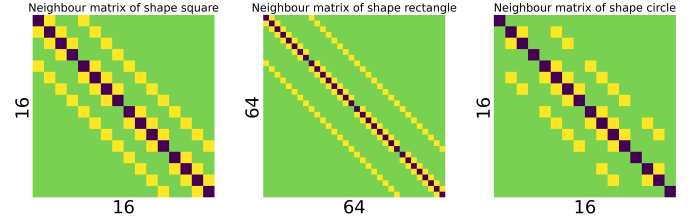
where x represents the position, v the velocity, k the spring constant, and m the mass of the object. The first derivative of position in time is the velocity, and the first derivative of velocity is the acceleration.

These equations are derived by combining Newton's second law, which tells us that force is directly proportional to the mass times acceleration, and Hooke's law, which states that the restoring force of a spring is given by $F = -kx$.

III. METHOD

To discretize the different membranes, each shape was flattened into a vector, whereby the neighbourhood was preserved. Derived from equation 2, this resulted into:

$$\frac{u_{i+1,j} + u_{i-1,j} + u_{i,j+1} + u_{i,j-1} - 4u_{i,j}}{h} = Kv(i, j) \quad (7)$$

Fig. 2: Discretization of the points and their positions of Figure 2, for $L = 4$.

Where $v(i, j)$ is the vector \mathbf{v} from equation 3 and the left-hand side becomes \mathbf{Mv} . An example of these discretizations can be seen in Figure 2.

To optimize algorithmic performance, a sparse matrix representation was used for the input data. The discretization of this was used to calculate the eigenvalues, eigenfrequencies, and associated eigenvectors. To calculate this we used the `eigs` function from SciPy's `sparse.linalg` module.

To solve the time component, the selected eigenmodes were multiplied by equation 4 as specified by equation 1, where $t \in [0, 10]$ with a step size of 0.1.

In order to find the concentration of the steady-state solution of a given membrane, a direct method was implemented to solve the system. Whereas previously a system of $Mv = Kv$ is solved at each iteration, we now will solve $Mb = c$. Previously, we assumed that $c = 1$, whereas we are solving directly for it. We are now also exclusively focussing on the circle shape, as it features the more interesting set of boundary conditions. This means that we are constructing a stencil matrix for ∇^2 , in the same way as described in the initial part of the methods section. This involves the same discretisation method as used previously. Due to the relatively lower computational power needed to compute and solve the system, we opted to run the concentration solution on a matrix of length $L = 150$.

We construct the stencil matrix in the same fashion that we would for the iterative method. Then, the boundary conditions are applied, meaning that all points of the matrix that lie outside of the circular boundary, whose diameter spans the length of the matrix, are set equal to zero, as we do not want these points to influence the diffusion. The circle is centred on the origin $(0, 0)$, and we implement a diffusive source at the point $(0.6, 1.2)$ where the concentration equals 1, and acts as the source of the diffusion across the membrane. This is represented in vector b , which equals 0 except at the source of $(0.6, 1.2)$. We then solve $Mc = -b$ for concentration $c(x, y)$ by using the library method `scipy.sparse.linalg.spsolve()`.

To solve the harmonic oscillator equations, we employ

a second-order method called the Leapfrog method. We use the scheme as described by equations 27 and 28 in the assignment sheet, always evaluating position at a full step n , and velocity at half step $n + 1/2$:

$$x_{n+1} = \Delta t v_{n+1/2} + x_n \quad (8)$$

$$v_{n+3/2} = -\Delta t \frac{kx_{n+1}}{m} + v_{n+1/2} \quad (9)$$

where $x_n = x(t = n\Delta t)$ and $v_{n+1/2} = v(n + \frac{1}{2})\Delta t$.

As initial conditions, we take $x_0 = 1$. To determine the velocity at the half step, $v_{1/2}$, we rearrange equation 28 from the assignment sheet with $n = -1$, yielding:

$$v_{1/2} = \Delta t \frac{F(x_0)}{m} + v_{-1/2} \quad (10)$$

The ghost node $v_{-1/2}$ can be eliminated by noting that the oscillator is at rest at $t = 0$, $v_0 = 0$. Using a second-order approximation of the boundary node as the average of $v_{1/2}$ and $v_{-1/2}$ as

$$0 = v_0 \approx \frac{1}{2}(v_{1/2} + v_{-1/2}) \quad (11)$$

Solving for $v_{-1/2}$ and substituting back to 10, we get

$$v_{1/2} = \Delta t \frac{F(x_0)}{2m} \quad (12)$$

Using this approximation, we preserve the second-order accuracy of this numerical method.

We solve the equations with a default step size $\Delta t = 0.01$. At each iteration, we first solve for x_{n+1} using the value of x and v solved in the previous iteration, and then for $v_{n+3/2}$ using the last value of v and the newly computed value of x_{n+1} .

We examine different values of the spring constant k , keeping the weight constant $m = 1$ fixed. We also try different step sizes and compare our solution with the analytical solution by comparing the values of our solution and the analytical solution at the grid points $n\Delta t$ for position and $(n + \frac{1}{2})\Delta t$ for velocity. The analytical solution is given by

$$x(t) = A \sin(\omega t + \varphi) = \sin(\omega t + \frac{\pi}{2}) \quad (13)$$

$$v(t) = A\omega \cos(\omega t + \varphi) = \omega \cos(\omega t + \frac{\pi}{2}) \quad (14)$$

where $\omega = \sqrt{k/m}$, and A is the amplitude which is the same as x_0 , that is, in our case $A = 1$.

Lastly, we introduce an external time-dependent sinusoidal driving force to the oscillator as described in equation 29 of the assignment sheet, and take $F(t) = F_0 \sin(\omega_{drive}t)$. We then update $v_{n+3/2}$ in our scheme to

$$v_{n+3/2} = \Delta t \frac{(F_0 \sin(\omega_{drive}n\Delta t) - kx_{n+1})}{m} + v_{n+1/2} \quad (15)$$

The first eigenvector(s) for different shapes with $L = 1$

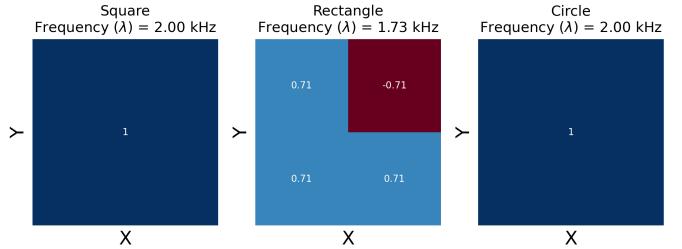
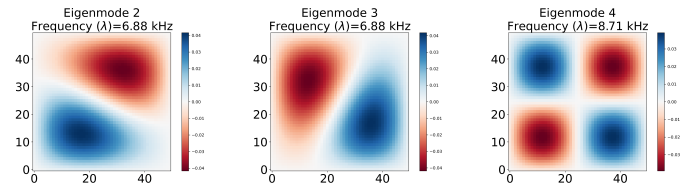
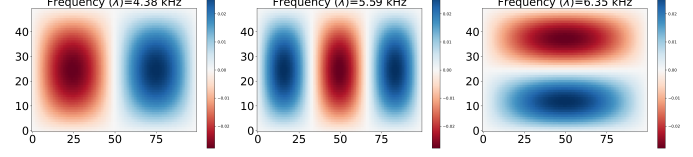


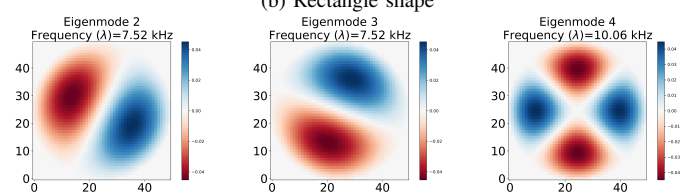
Fig. 3: Plot of the eigenvectors v for some of the smallest eigenvalues, using $L = 1$.



(a) Square shape



(b) Rectangle shape



(c) Circle shape

Fig. 4: The eigenmodus for three of the outputs, for $L = 50$. Red are negative values, whereby blue are the positive ones. The first eigenmodus is not shown, because its approximate the same figure for all three shapes.

Throughout our analysis, we set $F_0 = 0.5$ and investigate various values of ω_{drive} as multiplies of ω .

IV. RESULTS

WHEN solving the eigenvalue problem with $L = 1$, a simple matrix will be visible where both the circle and the square only have one eigenvector of length one. In contrast to this, the rectangle shape has two eigenvectors of length two, resulting in a larger grid as seen in Figure 3.

To get a better idea about how the eigenmodus will change, a $L = 50$ has been selected as seen in Figure ???. As seen here these images are symmetrically divided,

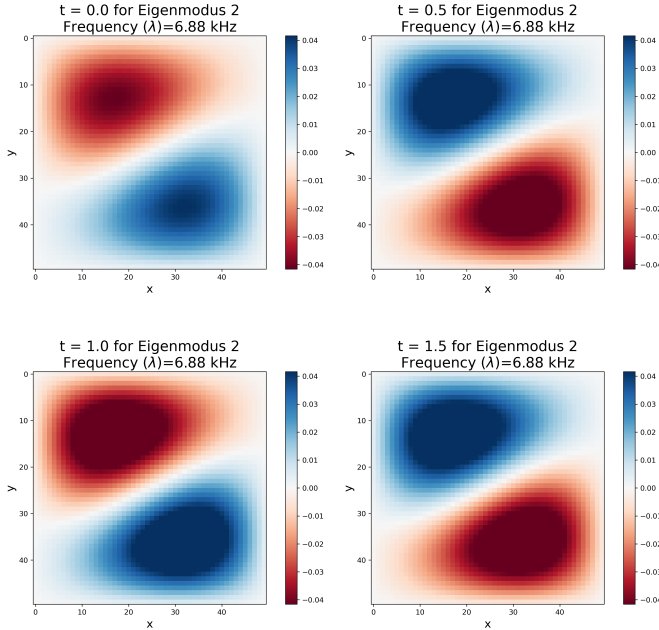


Fig. 5: Evolution of the eigenmodus over time, when including the time dependent solution.

whereby the positive values will oscillate up, and the negative values will oscillate down. This behaviour results in a wave-like pattern when plotting it over time, using equation 1 and 4, as seen in Figure 5.

Figure 6 shows how the mean eigenfrequency of all the eigenmodus changes when L is increased. As L increases, the resolution of the shape increases as well. This is because of the eigenvector being larger and capturing more information. The shift in colour is due to the the values sometimes being positive or negative, but the overall shape stays the same. As seen in this Figure ?? around $L = 80$ the frequency will converge at a value of 4.40 kHz for the square. Hereby the largest jump can be found in the beginning of the plot, between $L = 10$ and $L = 30$. At this point the frequency jumps from its lowest state to approaching the equilibrium point.

For the result of the concentration plots, we produced two graphs. We plot both the sources at $(0, 0)$ and $(0.6, 1.2)$, which allows us to study how the sum of the concentration varies. Figure 7 demonstrates how the diffusion behaves when the source is placed at the centre of the grid, as opposed to the off-centre placement. We can observe that the steady-state solution of the off-centre source reached the boundary faster than the control, meaning that some concentration reaches the Dirichlet boundary and is therefore lost in the system. This is corroborated by the total concentration of the circle for the off-centre being $\sum_{i=1}^n C_i \approx 0.55$. Comparatively, the centred diffusion was found to be ≈ 1 , confirming that

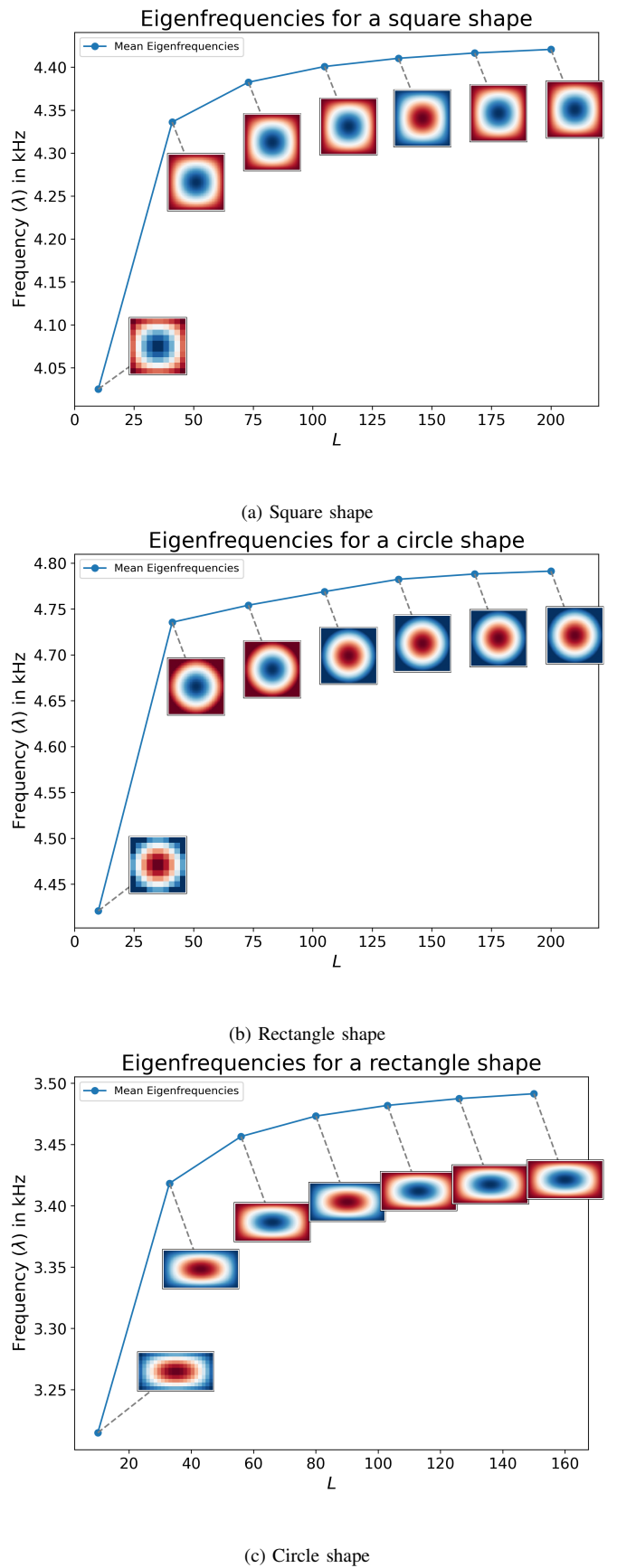
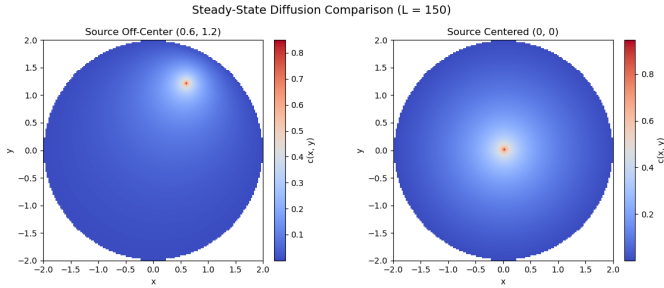
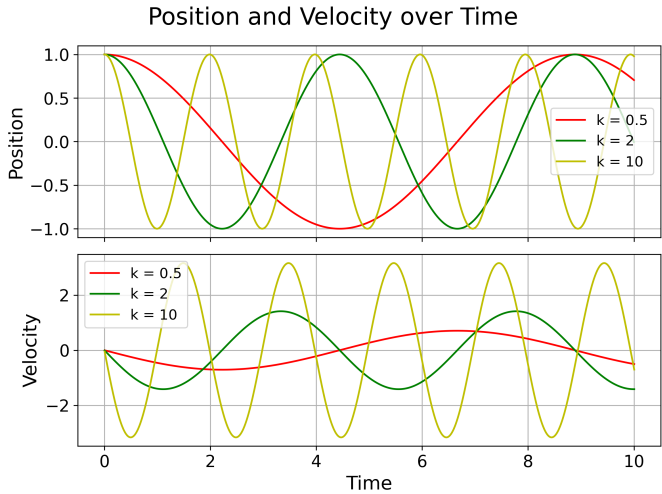


Fig. 6: Plot of the mean eigenfrequencies depending on the size of L , with an image of eigenmodus 1 to see the evolution of the figure. The mean is calculated over the different eigenmodus.

Fig. 7: Concentrations $c(x, y)$, for varying source points. $L = 150$ Fig. 8: Position and velocity over time for various spring constants k , $\Delta t = 0.01$ and total time $T = \#\text{steps} \cdot \Delta t = 10$.

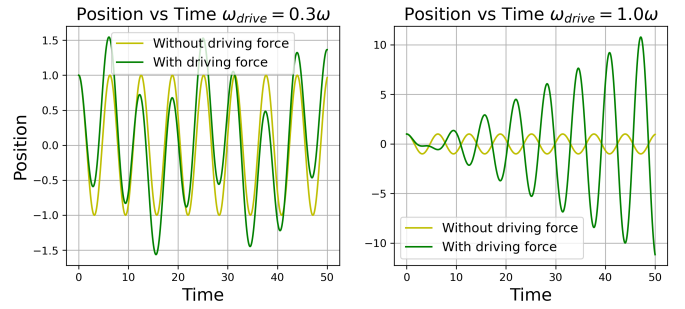
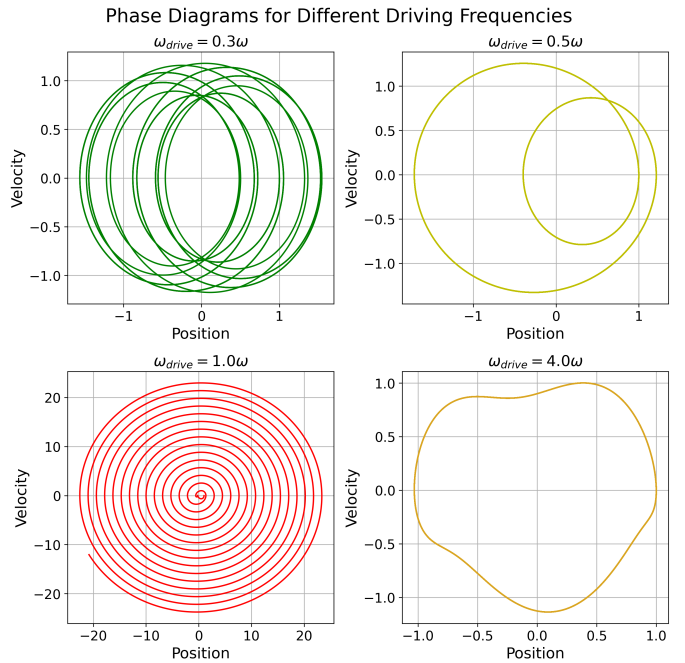
the implementation behaved as expected.

Figure 8 shows the solution to our oscillator equation, i.e. the position and velocity over time for three different values of spring constant k , $\Delta t = 0.01$ and total time $T = 10$.

Figure 9 shows the position over time for two different frequencies and $k = 1$, $\Delta t = 0.01$, and $T = 50$. And finally, Figure 10 shows phase plots (x, v) for four different frequencies. The frequencies are chosen as multiples of the system's original frequency and $k = 1$, $\Delta t = 0.01$, and $T = 100$.

V. DISCUSSION

AS $L \rightarrow 200$, the eigenfrequencies converge to approximately 4.40 kHz for the square shape, 3.50 kHz for the rectangle, and 4.75 kHz for the circle. This indicates that as L increases, the frequency approaches a stable equilibrium, giving us the answer to the first research question. Because of the size of the matrix, it wasn't possible to get an $L = 200$ for the rectangle without crashing the program. Because of this the rectangle plot has a maximum of $L = 150$, and thus shows different values

Fig. 9: Position over time for various ω_{drive} , for $F_0 = 0.5$, $k = 1$, $\Delta t = 0.01$ and $T = \#\text{steps} \cdot \Delta t = 50$.Fig. 10: Phase plots of (v, x) for various ω_{drive} , for $F_0 = 0.5$, $k = 1$, $\Delta t = 0.01$ and $T = \#\text{steps} \cdot \Delta t = 100$.

Based on Figure 5 one can see that the eigenmodus fluctuate between going up and down over time, resulting in the wave-like pattern we mentioned before. Different parts of the membrane influence each other, giving us this oscillation behaviour.

For the calculation of these eigenmodus, it was assumed that $h = 1/L$, but other spatial steps could be chosen, resulting in different figures and possibilities of numerical errors. The same can be said about A and B for equation 4, as for this report the assumption was made that $A = 1$ and $B = 1$, as mentioned before. When setting $A = 2$ and $B = 1.5$ we will get the same shape but the minimum and maximum values of the eigenvector are much larger and have a larger area, resulting in the shaping having darker colours.

We find from Figure 7 that the diffusion behaves as expected. Given the Dirichlet boundary conditions, we

find that some concentration gets lost on the boundary for the off-centre source. This could inform strategies for optimising heat or electrostatic potential, in that ideally one conserves as much of the initial energy as possible. The Dirichlet boundary here reflects the assumption that all energy that reaches the boundary simply dissipates; however, this assumption does not capture real-life physical settings. For example, the drum membrane, which served as the backdrop for the eigenvalue investigation, would certainly not behave in a strictly Dirichlet manner, which would lose energy to the physical, tensile, and sonic dimensions in the process. This is corroborated by the fact that the summed concentration for the off-centre system equalled about half of the centred system.

From Figure 8, we see that both position and velocity behave in a sinusoidal manner, as expected. The amplitude remains constant, while the frequency increases with k which can be explained by the analytical solution as described in equations 13 and 14.

The angular frequency is given by $\omega = \sqrt{\frac{k}{m}}$ and the period and frequency of the oscillator are given by $T = 2\pi/\omega$ and $f = 1/T$ respectively (note that T here is not the same as the T used in our simulation to describe the total time).

We can also see that the amplitude for position is $A = 1$ which is due to the initial condition, but for velocity, it is given by $A\omega$ which in our case is ω . Therefore, the amplitude of velocity increases with the spring constant k , i.e. for higher k , the object is moving faster.

Since the leapfrog method is a symplectic integrator and it conserves energy over long simulation times, we can simulate for many steps and we will continue seeing the same curve with only small errors from the analytical solution.

Figure 10 shows the phase plots of position vs velocity for different driving frequencies. We can see that when the driving frequency is the same as the original frequency, we get an unstable system and both the position and velocity keep increasing over time. This can also be seen in Figure 9. The solution is still a sinusoidal-like wave with the same period and frequency, but the amplitude is amplified.

For smaller frequencies, we see more chaotic, but still stable and periodic behaviour. For higher frequencies, we can see that the solution is modified only slightly. If there was no driving force, the phase plot would be a perfect circle. Note that the axes are not the same for all the plots.

REFERENCES

- [1] E. ÅKERVIK, J. HÖPFNER, U. EHRENSTEIN, and D. S. HENNINGSON, “Optimal growth, model reduction and control in a separated boundary-layer flow using global eigenmodes,” *Journal of Fluid Mechanics*, vol. 579, p. 305–314, 2007.